

New Insight into the Gas-Phase Bimolecular Self-Reaction of the HOO Radical

Josep M. Anglada,^{*,†} Santiago Olivella,^{*,†} and Albert Solé[‡]

Institut d'Investigacions Químiques i Ambientals de Barcelona, CSIC, Jordi Girona 18-26, 08034-Barcelona, Catalonia, Spain, and Centre Especial de Recerca en Química Teòrica i Departament de Química Física, Universitat de Barcelona, Martí i Franquès 1, 08028-Barcelona, Catalonia, Spain

Received: October 17, 2006; In Final Form: January 4, 2007

The singlet and triplet potential energy surfaces (PESs) for the gas-phase bimolecular self-reaction of HOO•, a key reaction in atmospheric environments, have been investigated by means of quantum-mechanical electronic structure methods (CASSCF and CASPT2). All the reaction pathways on both PESs consist of a first step involving the barrierless formation of a prereactive doubly hydrogen-bonded complex, which is a diradical species lying about 8 kcal/mol below the energy of the reactants at 0 K. The lowest energy reaction pathway on both PESs is the degenerate double hydrogen exchange between the HOO• moieties of the prereactive complex via a double proton transfer mechanism involving an energy barrier of only 1.1 kcal/mol for the singlet and 3.3 kcal/mol for the triplet at 0 K. The single H-atom transfer between the two HOO• moieties of the prereactive complex (yielding HOOH + O₂) through a pathway keeping a planar arrangement of the six atoms involves a conical intersection between either two singlet or two triplet states of A' and A'' symmetries. Thus, the lowest energy reaction pathway occurs via a nonplanar *cisoid* transition structure with an energy barrier of 5.8 kcal/mol for the triplet and 17.5 kcal/mol for the singlet at 0 K. The simple addition between the terminal oxygen atoms of the two HOO• moieties of the prereactive complex, leading to the straight chain H₂O₄ intermediate on the singlet PES, involves an energy barrier of 7.3 kcal/mol at 0 K. Because the decomposition of such an intermediate into HOOH + O₂ entails an energy barrier of 45.2 kcal/mol at 0 K, it is concluded that the single H-atom transfer on the triplet PES is the dominant pathway leading to HOOH + O₂. Finally, the strong negative temperature dependence of the rate constant observed for this reaction is attributed to the reversible formation of the prereactive complex in the entrance channel rather than to a short-lived tetraoxide intermediate.

1. Introduction

The hydroperoxy radical (HOO•) is a key transient intermediate in the combustion of hydrocarbon fuels, atmospheric photolysis cycles, and biochemical processes. In particular, the gas-phase bimolecular self-reaction of HOO• plays an important role in atmospheric chemistry,¹ but also in the oxidation reactions with ozone and oxygen² or biochemical systems.³ This reaction has been shown^{4–11} to be dominated by the formation of hydrogen peroxide (HOOH) plus molecular oxygen (O₂) (eq 1) and is a key process controlling steady-state concentrations of HO_x radicals in the troposphere, as well as the main source of HOOH in the atmosphere.¹²



The kinetics of reaction eq 1 has been extensively studied experimentally^{4–6,13–27} and computationally (RRKM modeling studies)^{19,28,29} for a wide range of temperatures and pressures. The rate constant for reaction of eq 1 in the gas phase at 298 K and 1 atm pressure is about $3 \times 10^{-12} \text{ cm}^3 \text{ molecule}^{-1} \text{ s}^{-1}$.^{1b,30} The temperature dependence of reaction of eq 1 has been investigated by several groups,^{4,8,15,16,18–24} and these studies all

observed strong negative temperature dependence; namely, the rate constant decreases with temperature. At around room temperature, the rate constant also shows a pressure dependence, increasing by a factor of ~ 2 between 10 and 1000 mbar at 298 K. This pressure and temperature dependence is attributed to a mechanism involving the formation of a short-lived intermediate, H₂O₄, which can either dissociate into the reactants or react to form the stable products. However, the nature of the postulated H₂O₄ intermediate is still uncertain and is open to speculation. An additional unresolved question concerns the electronic state of the H₂O₄ intermediate. When two HOO• molecules in their electronic ground state (²A'') combine, the spin state of the overall system they form can be either a singlet spin state or a triplet one. However, if one assumes that the products of reaction eq 1 are formed in their electronic ground state, namely singlet HOOH (¹A) plus triplet molecular oxygen (O₂, ³Σ_g⁻), designated by ³O₂, then these products can only be reached on the triplet potential energy surface (PES). This arises the question of whether H₂O₄ is a bound-triplet-state species, which may be possible for a hydrogen-bonded species where the unpaired electrons would not be required for bonding or whether the formed products are singlet HOOH (¹A) and excited singlet molecular oxygen (O₂, ¹Δ_g), designated by ¹O₂.

The geometrical structure, energetics, and vibrational frequencies of the H₂O₄ intermediate was investigated in detail by Fitzgerald and Schaefer³¹ by means of quantum mechanical calculations at the self-consistent field (SCF) level of theory with double-ζ (DZ) and double-ζ plus polarization (DZP) basis

* Corresponding author. E-mail: sonqtc@cid.csic.es (S.O.) and anglada@iiqab.csic.es (J.M.A.).

[†] Institut d'Investigacions Químiques i Ambientals de Barcelona.

[‡] Centre Especial de Recerca en Química Teòrica i Departament de Química Física.

sets. It was found that a straight covalently-bonded closed-shell chain of C_1 symmetry with HOOOH connectivity was more stable than a cyclic dimer $(HO_2)_2$ consisting of two HOO• radicals hydrogen-bonded head to tail in a planar six-membered-ring of C_{2h} symmetry with the two unpaired electrons loosely coupled to an overall triplet state of B_u symmetry. One six-membered-ring dimer structure showing a geometry essentially identical to that of 3B_u but with the two unpaired electrons loosely coupled to an open-shell of B_u symmetry was also located at the two-configuration SCF wave function and found to be energetically nearly degenerate with that triplet.³¹ By using Davidson-corrected configuration interaction singles and doubles (CISD) single point energy calculations at the SCF/DZP optimized geometries, Fitzgerald et al.³² also found that the C_1 chain and C_{2h} ring structures were bound by 9.9 and 8.6 kcal/mol, respectively, with respect to dissociation into two HOO• radicals. The question of the most stable form of H_2O_4 intermediate was reinvestigated later by Schaefer and co-workers,³³ using extensive basis sets and electron correlation methods. This agreed with their earlier study and showed that the global minimum is a closed-shell chain structure of C_1 symmetry. At the highest level of theory, namely, coupled cluster singles doubles and triples (CCSD(T)) with a triple- ζ plus double polarization and additional f-polarization basis set and including the zero-point vibrational energy (ZPVE) correction, the C_1 chain lies 1.6 kcal/mol below the planar C_{2h} cyclic doubly hydrogen-bonded structure.

In a subsequent theoretical work by Zhu and Lin,³⁴ the hybrid density functional theory (DFT) B3LYP method with the 6-311G(d,p) basis set was employed to investigate both the singlet and triplet PESs for the gas-phase bimolecular self-reaction of HOO•. The energies were calculated employing the G2M(CC5) model chemistry,³⁵ which uses a series of calculations with the B3LYP/6-311G(d,p) optimized geometry to approximate the CCSD(T)/6-311+G(3df,2p) level of theory including a "higher level correction (HLC)". The results showed that the singlet H_2O_4 chain-structure with C_1 symmetry is the most stable intermediate, which lies 19.1 kcal/mol below the energy of two HOO• radicals. Furthermore, the planar six-membered-ring structure with two hydrogen bonds and the two unpaired electrons coupled to the 3B_u triplet state was calculated to be bound by 9.5 kcal/mol with respect to dissociation into two HOO• radicals. By using the spin-unrestricted version of the B3LYP method (UB3LYP), Zhu and Lin located a singlet six-membered-ring doubly hydrogen-bonded structure of C_{2h} symmetry. At the G2M(CC5) level, the energy of this singlet is 0.1 kcal/mol lower than that of the corresponding triplet state. The calculations showed that the most favored product channel, producing HOOH + 3O_2 , occurs by the formation of the triplet six-membered-ring complex followed by direct H-atom transfer between the two HOO moieties via a transition state lying about 0.5 kcal/mol below the energy of two HOO• radicals. At this point we note that because of the self-interaction error of the DFT methods the H-atom transfer between two HOO• radicals cannot be correctly described.³⁶ As regards the hypothetical formation of HOOH + 1O_2 , Zhu and Lin found four channels over the singlet PES. All the transition states associated with these channels were calculated to lie above the reactants by 2.8–5.6 kcal/mol at the G2M(CC5) level. However, taking into account the expected multireference character of the wave function of various stationary points on the singlet PES, the predictions based on single-determinant B3LYP calculations are at least questionable. Furthermore, Zhu and Lin assumed that the formation of the H_2O_4 chain-structure intermediate is a

barrierless process involving the simple addition between the terminal oxygen atoms of the two HOO• radicals. Therefore, no transition structure was searched for this process.

Recently, Donaldson and Francisco³⁷ have located various stationary points on the triplet PES connecting 3O_2 + HOOH with two HOO• radicals using quadratic configuration interaction with singles doubles (QCISD) calculations in conjunction with the 6-311G(2df,2p) basis set. The energies were obtained at the QCISD with a perturbative treatment of triple excitations (QCISD(T)) level using the 6-311++G(3df,3pd) basis set and the QCISD/6-311G(2df,2p) optimized geometries. For the reaction reverse of reaction eq 1, these authors predict a mechanism that consists in a simple hydrogen abstraction, with a barrier of 35.5 kcal/mol, followed by formation of a six-membered complex with two hydrogen bonds, which breaks up into two HOO• radicals. Regarding the singlet PES connecting 1O_2 + HOOH with two HOO• radicals, Donaldson and Francisco have not reported any stationary point.

We feel that the conclusions drawn from the theoretical calculations of Zhu and Lin concerning the reaction pathways on the singlet PES of the HOO• self-reaction merit further study. With this purpose, here we report the results of multireference second-order perturbative energy calculations carried out on the geometries pertaining to the reaction pathways explored on both the singlet and triplet PESs of the HOO• + HOO• reaction, in a continued effort to elucidate the mechanism of this important reaction.

2. Computational Methods

The geometries of the relevant stationary points on the lowest energy singlet and triplet PESs of the HOO• + HOO• reaction system, were optimized by use of multiconfiguration self-consistent field (MCSCF) wave functions of the complete active space (CAS) SCF class³⁸ with the triple split-valence 6-311+G(3df,2p) basis set³⁹ (which includes a single diffuse sp shell,⁴⁰ triple d-polarization, and a single additional f-polarization on heavy atoms and double p-polarization on hydrogen atoms) employing analytical gradient procedures.^{41,42} The CAS of each stationary point was selected following the procedure suggested by Anglada and Bofill,⁴³ based on the fractional occupation of the natural orbitals generated from the first-order density matrix calculated from an initial multireference single- and double-excitation configuration interaction (MRDCI) wave function correlating all valence electrons. The CAS varied from two electrons in two molecular orbitals (MOs), labeled as (2,2), for HOOH to fourteen electrons in twelve MOs, labeled as (14,-12), for several stationary points. Thus, for HOO• the fractional occupancies of the natural orbitals indicated that there are five electrons in four MOs, labeled as (5,4): the σ , σ^* and π , π^* orbitals of the OO fragment. In the case of the products, the CAS of HOOH comprised the σ , σ^* orbitals of the OO fragment, whereas the CAS of O_2 comprised eight electrons in six MOs, labeled as (8,6), which included the σ_z , σ_z^* and π_x , π_x^* and π_y , π_y^* orbitals of the OO bond.

All the stationary points were characterized by their harmonic vibrational frequencies as minima or saddle points. The harmonic vibrational frequencies were obtained by diagonalizing the mass-weighted Cartesian force constant matrix calculated at the CASSCF/6-311+G(3df,2p) level. Connections of the transition structures between designated minima were confirmed in each case by IRC calculations⁴⁴ at the latter level of theory using the second-order algorithm of Gonzalez and Schlegel.⁴⁵ Zero-point vibrational energies (ZPVEs) were determined from unscaled harmonic vibrational frequencies.

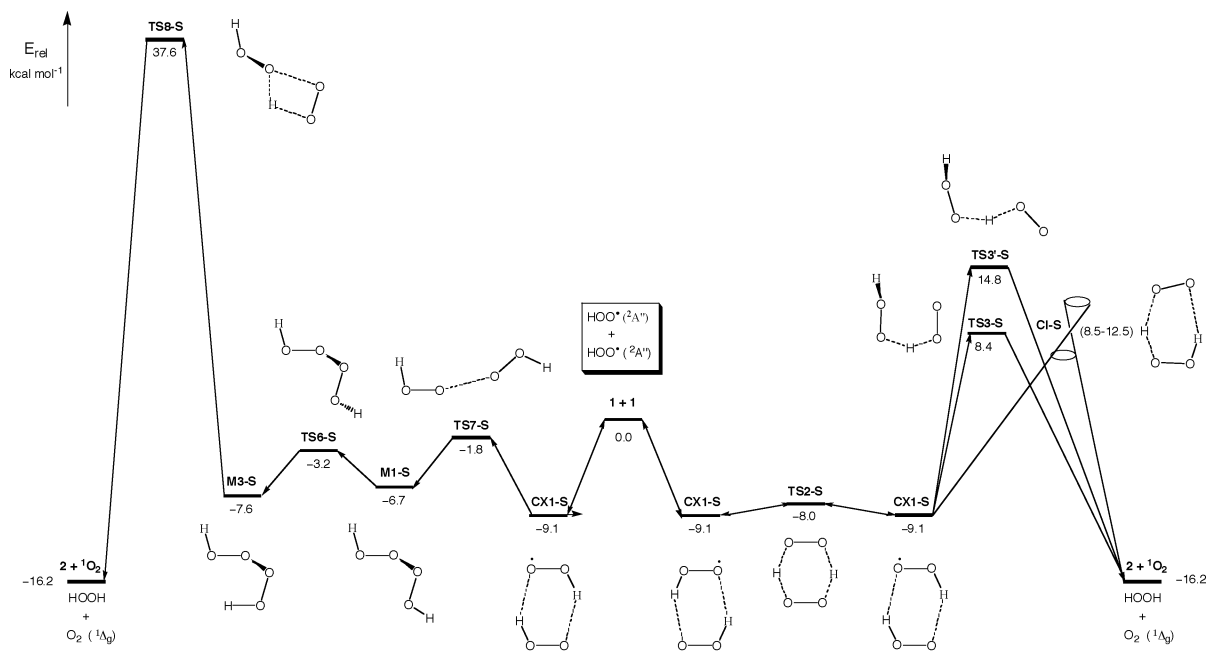


Figure 1. Schematic energy profiles showing the most relevant structures concerning the reaction pathways on the singlet potential energy surface for the self-reaction of HOO•. Relative energy values obtained from the ZPVE-corrected CASPT2/6-311+G(3df,2p) total energies. The CASPT2/6-311+G(3df,2p) relative energy was used for the conical intersection CI-S.

In addition to the study of the adiabatic reaction paths on the lowest energy singlet and triplet PESs, the regions where surface crossings between these PESs and those of low lying excited electronic states may occur were investigated. The lowest energy points on the crossing seam of singlet–singlet and triplet–triplet surface crossings (conical intersections) were optimized at the CASSCF(14,12)/6-311+G(3df,2p) level of theory using the algorithm by Anglada and Bofill.⁴⁶

To incorporate the effect of dynamical valence-electron correlation on the relative energy ordering of the stationary points and conical intersections, second-order multiconfigurational perturbation theory calculations based on the CASSCF reference function (CASPT2)⁴⁷ were carried out with the 6-311+G(3df,2p) basis set. CASPT2/6-311+G(3df,2p) single point energies were calculated at the geometries optimized at the CASSCF/6-311+G(3df,2p) level and all valence electrons were correlated.

It is worth noting that at the CASSCF level of theory the energy difference between the crossing states at the conical intersections is calculated to be close to the expected value of zero kcal/mol, whereas at the CASPT2 level this energy difference rises to a few kcal/mol. This is due to the sensitivity of the optimum geometries of the conical intersections to the inclusion of dynamical valence-electron correlation and indicates that the usual computational strategy to perform single-point CASPT2 calculations at CASSCF optimized geometries may fail for these points. Unfortunately, the geometry optimization of conical intersections at the CASPT2 level are too costly at present even for systems such as H₂O₄. Therefore, we assumed that the value of the CASPT2 relative energy of a conical intersection ideally optimized at the CASPT2 level of theory lies within the range of values bound by the relative energies computed at this level of theory for the two crossing states using the CASSCF optimized geometry.

For the hydrogen-bonded complexes found in this work, the basis set superposition error (BSSE) was calculated at the CASPT2/6-311+G(3df,2p) level by using the counterpoise method of Boys and Bernardi.⁴⁸

To examine the characteristics of the bonding and interactions in the most relevant structures, we have also performed an analysis of the electronic charge density within the framework of the topological theory of atom in molecules (AIM).⁴⁹ The first-order electron density matrix obtained from the CASSCF/6-311+G(3df,2p) wave function was used in this analysis.

The CASSCF calculations were carried out by using the GAMESS⁵⁰ and MOLCAS-6⁵¹ program packages, whereas the CASPT2 computations were performed with the latter program package. The PROAIM and EXTREME programs of Bader et al.⁵² were used to carry out the AIM analysis of the electronic charge density.

Although this article focus on the reaction pathways on both the singlet and triplet PESs of the self-reaction of HOO•, rather than on the rate constants of this reaction, we have estimated the tunneling effect on the elementary reactions involving single or double H-atom transfer. According to Wigner,⁵³ the effect of tunneling on a reaction is to enhance the specific rate constant by a factor $\Gamma(T)$ given by

$$\Gamma(T) = 1 + \frac{1}{24} \left(\frac{h\nu^\ddagger}{kT} \right)^2 \quad (1)$$

where T is the absolute temperature, h is the Plank constant, k is the Boltzmann constant, and ν^\ddagger is the frequency of the imaginary mode of the transition state (written as $\nu^\ddagger i$).

3. Results and Discussion

Figures 1 and 2 display schematic energy profiles showing the most relevant structures concerning the reaction pathways on the singlet and triplet PES, respectively, calculated for the gas-phase bimolecular self-reaction of HOO•. The nomenclature used for labeling the structures is composed of two parts. The

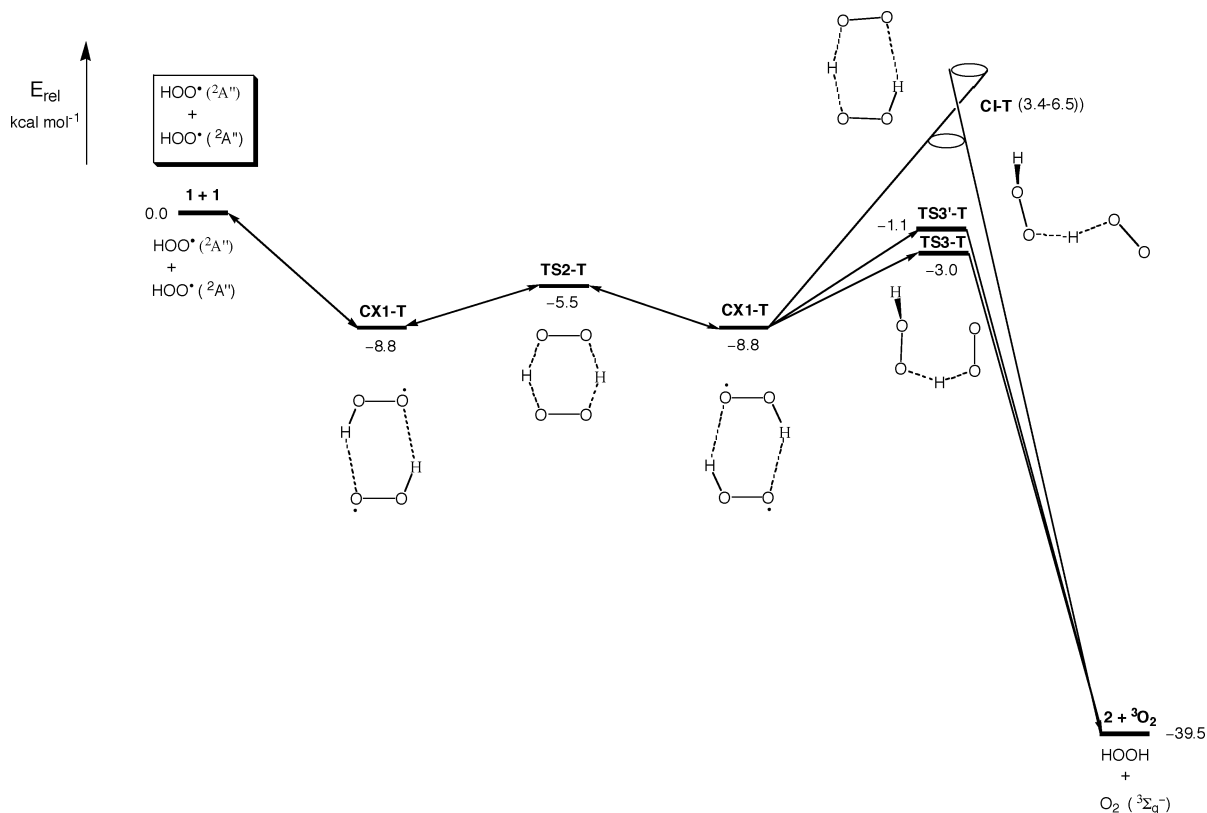


Figure 2. Schematic energy profiles showing the most relevant structures concerning the reaction pathways on the triplet potential energy surface for the self-reaction of HOO*. Relative energy values obtained from the ZPVE-corrected CASPT2/6-311+G(3df,2p) total energies. The CASPT2/6-311+G(3df,2p) relative energy was used for the conical intersection CI-T.

first part indicates the nature of the structure, namely, hydrogen-bonded complex (CX), intermediate (M), transition state (TS), and conical intersection (CI). The structures are distinguished from each other by appending the numbers 1, 2, etc., as they are introduced. The second part of the label designates the spin multiplicity of the electronic state, namely, singlet (S) or triplet (T). For example, CX2-T is the equilibrium structure of the second hydrogen-bonded complex on the triplet PES, M1-S is the equilibrium structure of the first intermediate on the singlet PES, and TS3-T is the third transition state on the triplet PES.

The Cartesian coordinates of all structures reported in this Article are available as Supporting Information. Total electronic energies computed at the CASSCF and CASPT2 levels of theory with the 6-311+G(3df,2p) basis set, as well as the ZPVEs, are collected in Table S1 (Supporting Information). Table 1 gives the energies of the most relevant structures, relative to the isolated reactants, computed at different levels of theory. Relative energies discussed in the text refer to values determined from the ZPVE-corrected CASPT2 energies, designated by CASPT2+ZPVE, unless stated otherwise. Finally, the approximate tunneling factor for the reactions involving single or double H-atom transfer are given in Table S2 (Supporting Information).

3.1. Reactants and Products. Selected geometrical parameters of the reactant HOO* (labeled as 1) and products HOOH, $^1\text{O}_2$, and $^3\text{O}_2$ (labeled as 2, $^1\text{O}_2$, and $^3\text{O}_2$, respectively) of reaction 1 are shown in Figure S1 (Supporting Information). It is worth noting that the geometries calculated for HOO* and HOOH compare well with results in the literature.⁵⁴ However, it should be emphasized that because of the lack of dynamic electron correlation effects the O–O bond lengths calculated at the CASSCF level of theory are always too long. The geometry of 1 (O–O = 1.350 Å, H–O = 0.947 Å, and H–O–O = 104.1°)

TABLE 1: Relative Energies (kcal/mol) Calculated with the 6-311+G(3df,2p) Basis Set for the Most Relevant Structures on the Lowest Singlet- and Triplet-State Potential Energy Surfaces for the HOO* + HOO* Reaction System^a

structure	symmetry	state	CASSCF(14,12)	CASPT2 ^b	CASPT2+ZPVE ^c
1 + 1			0.0	0.0	0.0
2 + $^3\text{O}_2$			-39.0	-40.3	-39.5
2 + $^1\text{O}_2$			-18.6	-16.9	-16.2
CX1-S	C_{2h}	$^1\text{B}_g$	-5.9	-11.6 (-10.7)	-9.1 (-8.2)
CX1-T	C_{2h}	$^3\text{B}_g$	-5.9	-11.2 (-10.3)	-8.8 (-7.9)
CX2-S	C_1	^1A	-3.3	-6.0 (-5.1)	-4.5 (-3.6)
CX2-T	C_1	^3A	-3.3	-5.8 (-4.9)	-4.3 (-3.4)
TS1-S	C_1	^1A	-2.9	-4.8	-5.1
TS1-T	C_1	^3A	-2.9	-4.6	-4.8
TS2-S	D_{2h}	$^1\text{B}_{2u}$	21.1	-6.4	-8.0
TS2-T	D_{2h}	$^3\text{B}_{2u}$	23.6	-3.8	-5.5
CI-S	C_s	$^1\text{A}'$	29.3	8.5	
CI-S	C_s	$^1\text{A}''$	29.6	12.5	
CI-T	C_s	$^3\text{A}'$	23.8	6.5	
CI-T	C_s	$^3\text{A}''$	24.1	3.4	
TS3-S	C_1	^1A	23.0	9.9	8.4
TS3-S	C_1	^1A	28.8	17.0	14.8
TS3-T	C_1	^3A	14.2	-0.6	-3.0
TS3-T	C_1	^3A	15.1	1.5	-1.1
M1-S	C_2	^1A	-3.7	-9.5	-6.7
M2-S	C_2	^1A	-4.2	-10.0	-7.2
M3-S	C_1	^1A	-4.7	-10.5	-7.6
TS4-S	C_s	$^1\text{A}'$	3.5	-1.1	1.8
TS5-S	C_1	^1A	-2.2	-7.2	-5.1
TS6-S	C_1	^1A	-0.6	-5.9	-3.2
TS7-S	C_2	^1A	-0.7	-3.1	-1.8
TS8-S	C_1	^1A	48.0	38.9	37.6

^a The values given in parentheses include the basis set superposition error correction for the CX1-S, CX2-S, CX1-T, and CX2-T complexes.

^b Calculated using the geometries optimized at the CASSCF level.

^c Relative CASPT2 energies including the zero-point vibrational Energy correction.

agrees reasonably well with that (O–O = 1.335 Å, H–O = 0.971 Å, and H–O–O = 104.4°) calculated at the QCISD(T)/6-311G(2df,2p) level,⁵⁵ which is in remarkable agreement with

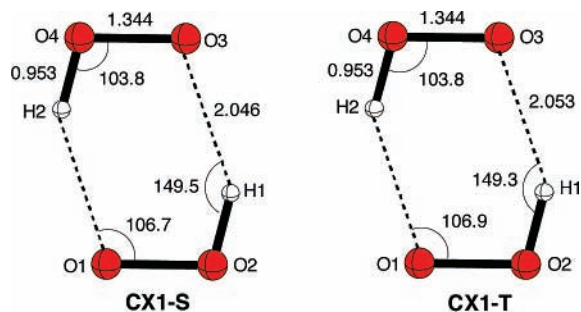


Figure 3. Selected geometrical parameters of the CASSCF/6-311+G-(3df,2p)-optimized geometries of the singlet (**CX1-S**) and triplet (**CX1-T**) doubly hydrogen-bonded complexes. Distances are given in Å and angles in deg.

the experimental geometry ($\text{O}-\text{O} = 1.331 \text{ \AA}$, $\text{H}-\text{O} = 0.971 \text{ \AA}$, and $\text{H}-\text{O}-\text{O} = 104.1^\circ$) reported by Lubic and Amano.⁵⁶ Concerning the product HOOH, the values of the geometrical parameters of **2** ($\text{O}-\text{O} = 1.478 \text{ \AA}$, $\text{H}-\text{O} = 0.943 \text{ \AA}$, $\text{H}-\text{O}-\text{O} = 99.9^\circ$, and $\text{H}-\text{O}-\text{O}-\text{H} = 118.0^\circ$) compare well with those ($\text{O}-\text{O} = 1.455 \text{ \AA}$, $\text{H}-\text{O} = 0.964 \text{ \AA}$, $\text{H}-\text{O}-\text{O} = 100.2^\circ$, and $\text{H}-\text{O}-\text{O}-\text{H} = 123.5^\circ$) calculated at the CCSD(T)/6-311G(d) level⁵⁴ and those of the experimental geometry ($\text{O}-\text{O} = 1.464 \text{ \AA}$, $\text{H}-\text{O} = 0.965 \text{ \AA}$, $\text{H}-\text{O}-\text{O} = 99.4^\circ$, and $\text{H}-\text{O}-\text{O}-\text{H} = 120.0^\circ$).⁵⁷ Finally, we note that the $\text{O}-\text{O}$ bond lengths of 1.227 and 1.214 Å of $^1\text{O}_2$ and $^3\text{O}_2$, respectively, are in good agreement with the experimental values of 1.22 and 1.21 Å.⁵⁸

According to Table 1, the self-reaction of HOO^\bullet leading to the formation of HOOH plus $^3\text{O}_2$ is predicted to involve an energy of reaction (designated by ΔU_r) of -40.3 kcal/mol . Inclusion of the thermal correction to enthalpy, obtained by assuming ideal gas behavior from the unscaled harmonic frequencies and moments of inertia by standard methods,⁵⁹ leads to an enthalpy of reaction at 298 K (designated by $\Delta H_r(298 \text{ K})$) of -39.6 kcal/mol , which is in reasonable agreement with the $\Delta H_f(298 \text{ K})$ of -38.2 kcal/mol derived from experimental enthalpies of formation.⁶⁰ Regarding the self-reaction of HOO^\bullet yielding $\text{HOOH} + ^1\text{O}_2$, it is predicted to involve a ΔU_r of -16.9 kcal/mol . Inclusion of the thermal correction to enthalpy leads to a $\Delta H_r(298 \text{ K})$ of -16.3 kcal/mol . Although the experimental value for this reaction is unknown, an estimate of -15.7 kcal/mol can be obtained from the $\Delta H_f(298 \text{ K})$ of -38.2 kcal/mol determined⁶⁰ for the self-reaction of HOO^\bullet leading to $\text{HOOH} + ^3\text{O}_2$ and the experimental $^3\text{O}_2-^1\text{O}_2$ energy gap of 22.5 kcal/mol .⁵⁸

3.2. Prereactive Hydrogen-Bonded Complexes. As it is not uncommon in many gas-phase reactions of interest in atmospheric chemistry, the bimolecular self-reaction of HOO^\bullet on both the singlet and triplet PESs begins with the barrierless formation of a prereactive loosely bound complex in the entrance channel. The optimized geometries of the lowest-energy singlet and triplet states of this complex, labeled as **CX1-S** and **CX1-T**, respectively, are shown in Figure 3. These nearly identical structures have C_{2h} symmetry and were characterized as a true local minimum on the corresponding PES. As compared with the bond distances in **1**, the HOO units of **CX1-S** and **CX1-T** show a 0.006 Å lengthening and a 0.006 Å shortening of the H–O and O–O bond distances, respectively. Interestingly enough, the AIM topological analysis of the electron charge density in **CX1-S** and **CX1-T** revealed the presence of a bond critical point between the atoms O1 and H2 and of another bond critical point between the atoms O3 and H1, indicating that there is a bonding interaction between these atom pairs. The low value of the electron charge density at these bond critical points (0.0193 and 0.0190 e bohr⁻³ for **CX1-S** and **CX1-T**, respectively), the

positive value of the its Laplacian (0.0779 and 0.0767 e bohr⁻⁵ for **CX1-S** and **CX1-T**, respectively), and the positive value of the local energy density⁶¹ (0.0017 and 0.0018 hartree bohr⁻³ for **CX1-S** and **CX1-T**, respectively) calculated for these bond critical points is typically associated with hydrogen-bond-like interactions. In addition, a ring critical point with a small electron charge density (0.0089 and 0.0088 e bohr⁻³ for **CX1-S** and **CX1-T**, respectively) was located in the middle of the six-membered-ring of both structures. These electronic features indicate the formation of two hydrogen bonds between the HOO moieties in **CX1-S** and **CX1-T**, which leads to a six-membered-ring equilibrium structure with two abnormally long H···O intermolecular distances (2.046 and 2.053 Å for **CX1-S** and **CX1-T**, respectively). It is to be mentioned that the geometries of the doubly hydrogen-bonded complexes LM6 and LM8 in ref 34, located at the UB3LYP/6-311G(d,p) level by Zhu and Lin, are qualitatively similar to those of **CX1-S** and **CX1-T**, respectively. However, the hydrogen-bond distances in the latter structures are significantly longer than in LM6 and LM8. The same trend is observed when the geometrical parameters of **CX1-T** are compared to those of the doubly hydrogen-bonded complex optimized at the QCISD/6-311G(2df,2p) level of theory reported by Donalson and Francisco.³⁷

An inspection of the CASSCF(14,12) natural orbitals obtained for **CX1-S** revealed the presence of two nearly singly occupied orbitals: one of a_u symmetry with electron occupancy of 0.9864 and one of b_g symmetry with electron occupancy of 1.0549. Basically, these singly occupied orbitals are the positive and negative combinations of the π -type orbitals (a'' symmetry) describing the unpaired electron of each isolated HOO^\bullet radical. Therefore, **CX1-S** is a doubly hydrogen-bonded species where the unpaired electrons of the two radical moieties are not used for bonding but are coupled to an overall open-shell singlet of B_u symmetry. Similarly, **CX1-T** has a natural orbital of a_u symmetry with electron occupancy of 1.0208 and an orbital of b_g symmetry with electron occupancy of 1.0203. Again, these singly occupied orbitals are the positive and negative combinations of the π -type orbitals describing the unpaired electron of each HOO^\bullet radical in the isolated reactants. Therefore, **CX1-T** is also a doubly hydrogen-bonded species where the unpaired electrons of the two radical moieties are coupled to an overall triplet of B_u symmetry. These electronic features indicate that **CX1-S** and **CX1-T** can be considered as the singlet and triplet states, respectively, of a doubly hydrogen-bonded diradical complex. We also note that in addition to the two singly occupied orbitals of a_u and b_g symmetry, **CX1-S** and **CX1-T** have two doubly occupied orbitals of a_u and b_g symmetry. Therefore, these complexes have a total of six π -type electrons.

According to Table 1, **CX1-S** and **CX1-T** lie 9.1 and 8.8 kcal/mol, respectively, below the energy of the isolated reactants. Inclusion of the correction for the BSSE leads to a stabilization energy of **CX1-S** and **CX1-T** toward decomposition into their components of 8.2 and 7.9 kcal/mol, respectively. It is worth noting that the BSSE-uncorrected energy (8.8 kcal/mol) of **CX1-T** relative to the separated reactants compares reasonably well with the values (8.6 and 9.5 kcal/mol) of earlier theoretical calculations.^{32,34}

In addition to the above doubly hydrogen-bonded diradical complex, we also found a one-hydrogen-bonded diradical complex. The optimized geometries of singlet and triplet states of this complex, labeled as **CX2-S** and **CX2-T**, respectively, are shown in Figure S2 (Supporting Information). Both structures were characterized as a true local minimum on the corresponding PES. As found for the doubly hydrogen-bonded

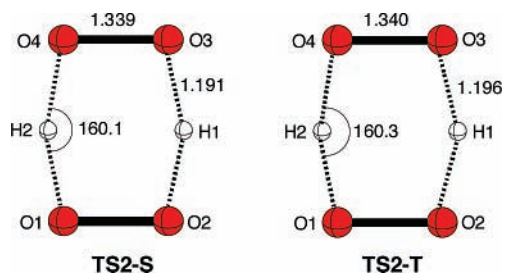


Figure 4. Selected geometrical parameters of the CASSCF/6-311+G-(3df,2p)-optimized geometries of the singlet (**TS2-S**) and triplet (**TS2-T**) transition structures for the double H-atom transfer in the **CX1-S** and **CX1-T** complexes. Distances are given in Å and angles in deg.

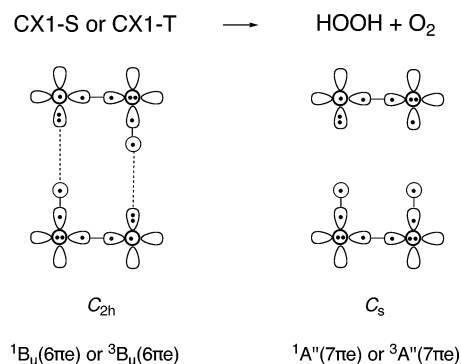
diradical complex, the geometrical parameters of **CX2-S** and **CX2-T** are nearly identical. These complexes lie 4.5 and 4.3 kcal/mol, respectively, below the energy of the isolated reactants (see Table 1). Inclusion of the correction for the BSSE leads to a stabilization energy of **CX2-S** and **CX2-T** toward decomposition into two HOO^\bullet radicals of 3.6 and 3.4 kcal/mol, respectively. At this point, it is worth noting that the geometry of the one-hydrogen-bonded complex LM7 in ref 34, optimized at the UB3LYP/6-311G(d,p) level, is qualitatively similar to that of **CX2-T**, though the $\text{H}\cdots\text{O}$ bond in the latter structure is significantly longer.

We found that the above doubly hydrogen-bonded and one-hydrogen-bonded complexes can isomerize to each other through the rotation of one HOO group along a hydrogen bond. The optimized geometries of the rotational transition structures for the isomerizations of **CX2-S** to **CX1-S** (labeled as **TS1-S**) and **CX2-T** to **CX1-T** (labeled as **TS1-T**) are shown in Figure S3 (Supporting Information). At the CASPT2 level, the energy barriers for these processes are calculated to be of only 1.2 kcal/mol (see Table 1). After inclusion of the ZPVE corrections, it turns out that **TS1-S** and **TS1-T** lie 0.6 and 0.5 kcal/mol below the energy of the complexes **CX2-S** and **CX2-T**, respectively. These results lessen the relevance of the one-hydrogen-bonded complexes **CX2-S** and **CX2-T** as compared to the energetically more stable doubly hydrogen-bonded complexes **CX1-S** and **CX1-T**.

3.3. Double H-Atom Transfer. As shown in Figures 1 and 2, after forming the prereactive doubly hydrogen-bonded complexes **CX1-S** and **CX1-T** on the singlet and triplet PESs, respectively, the lowest energy reaction pathway on both PESs is predicted to be the concerted transfer of two H-atoms between the two HOO^\bullet moieties, leading to the formation of an identical equilibrium structure of the same complexes. These degenerate reactions take place on the singlet and triplet PESs through the transition structures labeled as **TS2-S** and **TS2-T**, respectively, displayed in Figure 4, which have D_{2h} symmetry. Interestingly enough, the four interatomic distances between the hydrogen and oxygen atoms at these transition structures are notably short (~ 1.2 Å), indicating a strong hydrogen bonding interaction between these atoms. It is worth mentioning that none of these two transition structures were reported in earlier theoretical studies on the self-reaction of HOO^\bullet .

The natural orbitals calculated for **TS2-S** and **TS2-T** revealed in each case the presence of two nearly singly occupied orbitals: one of a_u symmetry and the other of b_{2g} symmetry, which are perpendicular to the plane containing the six atoms. Again, these singly occupied orbitals are the positive and negative combinations of the π -type orbitals describing the unpaired electron of each HOO^\bullet moiety. At the same time, the MOs of **TS2-S** and **TS2-T** describing the bonds involved in the double hydrogen exchange between the two HOO^\bullet moieties

SCHEME 1: Pictorial Representation of the Electronic Structure Features of the Doubly Hydrogen-Bonded Complex and the Reaction Products Resulting from a Single H-Atom Transfer



are found to lie on the plane containing the six atoms. Therefore, the unpaired electrons of **TS2-S** and **TS2-T** do not participate in the double hydrogen-exchange process but are coupled to an overall open-shell singlet or triplet of B_{2u} symmetry. These electronic features indicate that the double hydrogen exchange in **CX1-S** and **CX1-T** through the **TS2-S** and **TS2-T** transition states, respectively, correspond to a *double proton transfer* reaction pathway rather than a *double hydrogen atom transfer* mechanism.^{62,63}

Table 1 shows that **TS2-S** and **TS2-T** lie 8.0 and 5.5 kcal/mol, respectively, below the sum of the energies of the separated reactants and 1.1 and 3.3 kcal/mol above the energies of the **CX1-S** and **CX1-T** complexes, respectively. Therefore, the double proton transfer in these complexes involves a remarkably low-energy barrier. In addition, the calculated values of the Γ factor (see Table S2, Supporting Information) for the transition structures **TS2-S** and **TS2-T** (i.e., 5.94 and 6.14, respectively) indicate that the tunneling effect should enhance significantly the rate constant of double H-atom transfer in **CX1-S** and **CX1-T**.

3.4. Single H-Atom Transfer. First of all, we investigated the transfer of a single H-atom between the two HOO^\bullet moieties of the **CX1-S** and **CX1-T** complexes through a reaction pathway keeping a planar arrangement of the six atoms. Scheme 1 shows a pictorial representation of the electronic structure of the complexes and the resulting products ($\text{HOOH} + {}^1\text{O}_2$ or $\text{HOOH} + {}^3\text{O}_2$). Following the convention of Goddard et al.,⁶⁴ we have ignored the core orbitals 1s and 2s for oxygen, which are tightly bound and remain relatively unchanged as the atoms are brought together to form the molecules. The 1s orbital of the hydrogen atoms is represented by a thin circle, and the oxygen 2p orbitals perpendicular to the plane of the paper are represented by heavy circles. Dots indicate the number of electrons in each orbital, tie lines indicate the coupling of two singly occupied orbitals into a bonding pair, and dashed lines indicate hydrogen-bonding interactions. As noted above, the **CX1-S** and **CX1-T** structures possess C_{2h} symmetry, have a total of six π electrons, and correspond to an electronic state of B_u symmetry. If we assume a planar arrangement (C_s symmetry) of the HOOH and O_2 molecules, it follows that the reaction products have a total of seven π electrons and the overall system is either a singlet or triplet state of A'' symmetry. When the point group symmetry of both **CX1-S** and **CX1-T** is lowered from C_{2h} to C_s by considering only the symmetry plane containing the six atoms, then the symmetry of the electronic states of these structures becomes A' . Thus, within the common point group C_s the electronic states of **CX1-S** and **CX1-T** do not correlate with

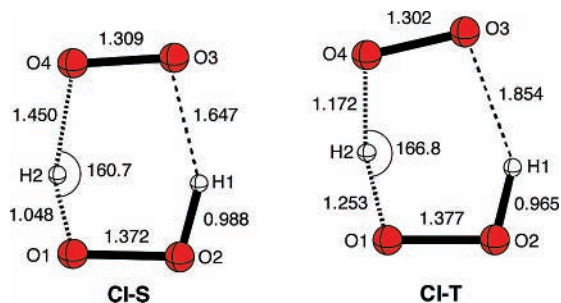


Figure 5. Selected geometrical parameters of the CASSCF/6-311+G-(3df,2p)-optimized geometries of the singlet–singlet (CI–S) and triplet–triplet (CI–T) conical intersections concerning the single H-atom transfer in the CX1–S and CX1–T complexes along a reaction pathway keeping a planar arrangement of the six atoms. Distances are given in Å and angles in deg.

those of the corresponding reaction products. As a consequence, the transfer of a single H-atom between the two HOO• moieties of CX1–S and CX1–T through a reaction pathway retaining the symmetry plane containing the six atoms is a nonadiabatic reaction. Therefore, such a C_s constrained reaction pathway must involve a surface crossing between the PESs of the A' and A'' states. In fact, a singlet–singlet and a triplet–triplet conical intersections, labeled as CI–S and CI–T, were located on these PESs.⁶⁵ Selected geometrical parameters of CI–S and CI–T are shown in Figure 5. The short interatomic distance O1–H2, as well as the long O3–H1 and O4–H2 distances, indicate that the conical intersection CI–S is closer to the reaction products ($2 + {}^1\text{O}_2$) than to the CX1–S complex. In contrast, the short O1–H2 and O4–H2 interatomic distances in CI–T suggest that the geometry of this structure is intermediate between the geometry of the CX1–T complex and that of the reaction products ($2 + {}^3\text{O}_2$).

At the CASPT2 level of theory, CI–S and CI–T are calculated to lie respectively 8.5–12.5 and 3.4–6.5 kcal/mol above the energy of the isolated reactants, but 20.1–24.1 and 14.6–17.7 kcal/mol above the energies of the CX1–S and CX1–T complexes, respectively (see Table 1). Therefore, the transfer of a single H-atom between the two HOO• moieties of both CX1–S and CX1–T through a reaction pathway retaining the planar arrangement of the six atoms involves a considerable energy barrier.

At this point, we note that single H-atom transfer between the two HOO• moieties of CX1–S and CX1–T could also take place along an adiabatic reaction pathway if the initial molecular symmetry of these structures is destroyed along the reaction pathway. This would allow an interaction between the electronic states of A' and A'' symmetries, which obviates the need for crossing and forces the correlation between the ground states of the reactants and products. In fact, we have found two nonplanar transition structures (C_1 symmetry) on the singlet PES, labeled as TS3–S and TS3'–S, and two nonplanar transition structures on the triplet PES, labeled as TS3–T and TS3'–T, for the transfer of a single H-atom in CX1–S and CX1–T, respectively (see Figure 6). In each case, these transition structures differ one from the other essentially in the relative orientation of the O1–O2 and O3–O4 bonds, TS3–S and TS3–T with both bonds in a *cisoid* position, and TS3'–S and TS3'–T with both bonds in a *transoid* position. Zhu and Lin have located at the B3LYP/6-311G(d,p) level a single transition structure (referred as TS12 in ref 34) for the transfer of a H-atom between the two HOO• moieties of a doubly hydrogen-bonded complex on the triplet PES (referred as LM8 in ref 34). Although such a transition structure shows a *cisoid* conformation, the O–H

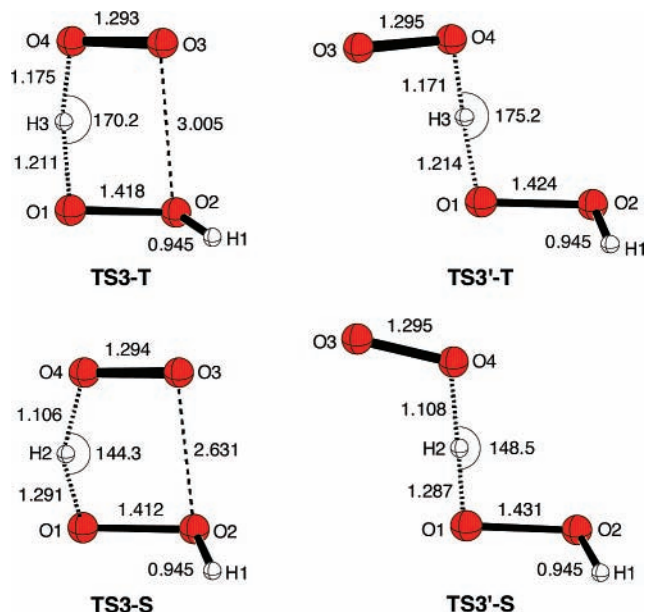


Figure 6. Selected geometrical parameters of the CASSCF/6-311+G-(3df,2p)-optimized structures of the singlet (TS3–S and TS3'–S) and triplet (TS3–T and TS3'–T) transition structures for a single H-atom transfer in the CX1–S and CX1–T complexes. Distances are given in Å and angles in deg.

distances of the breaking and forming bonds (1.075 and 1.377 Å) differ significantly from the values (1.175 and 1.211 Å) obtained for TS3–T. Regarding the QCISD/6-311G(2df,2p) calculations by Donalson and Francisco,³⁷ a single transition structure showing also a *cisoid* conformation has been reported for the same H-atom transfer on the triplet PES. The geometrical parameters of such a transition structure compare reasonably well with those of TS3–T.

As expected, the energies calculated at the CASSCF level of theory for TS3–S and TS3–T are considerably lower than those calculated for CI–S and CI–T, respectively (see Table 1). Furthermore, at all the levels of theory TS3–S and TS3–T are less energetic than TS3'–S and TS3'–T, respectively. As shown elsewhere,^{66,67} the lower energy of the transition structures with a *cisoid* arrangement of the O–O bonds, as compared to the energy of those with a *transoid* arrangement, is ascribed to a noncovalent O...O bonding interaction between the terminal oxygen atoms in the former transition structures.

According to last column of Table 1, a single H-atom transfer in CX1–S leading to the formation of $2 + {}^1\text{O}_2$ via TS3–S involves an energy barrier of 17.5 kcal/mol, whereas a single H-atom transfer in CX1–T yielding $2 + {}^3\text{O}_2$ through TS3–T involves an energy barrier of only 5.8 kcal/mol. Moreover, the latter transition state lies 3.0 kcal/mol below the energy of the separated reactants. It is worth mentioning that such an energy difference is significantly higher than the value of 0.5 kcal/mol obtained by Zhou and Lin³⁴ with the GM2(CC5) model chemistry but compares reasonably well with the value of 2.3 kcal/mol calculated by Donalson and Francisco³⁷ at the QCISD-(T)/6-311++G(3df,3pd) level of theory.

As expected for a H-atom transfer process, the calculated values of the Γ factor (see Table S2, Supporting Information) for the transition structures TS3–S, TS3'–S, TS3–T, and TS3'–T (i.e., 16.99, 30.69, 22.54, and 24.29, respectively) indicate that the tunneling effect should enhance substantially the rate constant of the reactions CX1–S \rightarrow $2 + {}^1\text{O}_2$ and CX1–T \rightarrow $2 + {}^3\text{O}_2$.

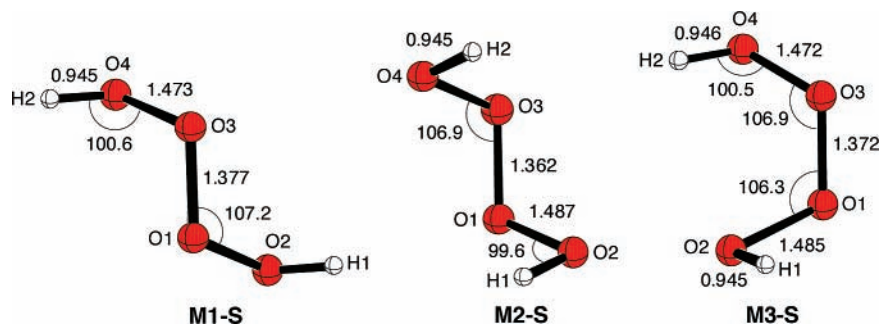


Figure 7. Selected geometrical parameters of the CASSCF/6-311+G(3df,2p)-optimized geometries of the three minima found for the H_2O_4 intermediate. Distances are given in Å and angles in deg.

3.5. Stepwise Mechanism. The straight covalently-bonded H_2O_4 adduct with the HOOOH connectivity was indeed found to be an intermediate on the singlet PES. For such a tetraoxide intermediate we located three minima arising from rotation of a HOO group along the newly formed O–O bond of the chain structure. The optimized geometries of these minima, labeled as **M1-S**, **M2-S**, and **M3-S** are shown in Figure 7. In agreement with earlier theoretical calculations,^{31–34} the global minimum of the H_2O_4 straight chain intermediate is found to be the structure of symmetry C_1 , namely **M3-S**. This structure lies 7.6 kcal/mol below the energy of the separated reactants. This value is in reasonable agreement with that (9.9 kcal/mol) obtained by Schaefer and co-workers³² from Davidson-corrected CISD calculations but is less than half the value (19.1 kcal/mol) determined by Zhu and Lin³⁴ by using the G2M(CC5) model chemistry. As regards the **M1-S** and **M2-S** structures, both have C_2 symmetry and are 0.9 and 0.4 kcal/mol, respectively, more energetic than the global minimum **M3-S**. These energy differences compare well with the G2M(CC5) values of 0.9 and 0.6 kcal/mol, respectively.³⁴

For the sake of completeness, the rotational transition structures for the interconversion between **M1-S** and **M2-S** (labeled as **TS4-S**), **M2-S** and **M3-S** (labeled as **TS5-S**), and **M1-S** and **M3-S** (labeled as **TS6**) were located on the singlet PES. The most important bond lengths and bond angles of these transition structures are displayed in Figure S4 (Supporting Information). The optimized geometries and relative energies of **TS4-S**, **TS5-S**, and **TS6-S** are found to be similar to those of the rotational transition structures calculated by using the UB3LYP/6-311G(d,p) and G2M(CC5) methods (referred as TS7, TS8, and TS9 in ref 34). Therefore, we skip the discussion on the geometry and relative energy of these transition structures.

As shown in Figure 1, the first step of the self-reaction of HOO^\bullet producing the H_2O_4 chain-structure intermediate is the formation of the **CX1-S** complex without surmounting an energy barrier. The second step is the simple addition between the terminal oxygen atoms of the two HOO^\bullet moieties of the complex leading to the **M1-S** structure. This step involves the passage through a transition structure of C_2 symmetry, labeled as **TS7-S**, whose optimized geometry is shown in Figure 8. The most remarkable geometrical feature of this transition structure is the long distance (2.560 Å) of the bond being formed between the oxygen atoms O1 and O3. As expected for the transition structure of a reaction involving the addition of two radicals (or the homolytic dissociation of the corresponding adduct), the wave function of **TS7-S** displayed a large amount of multireference character. In fact, an inspection of the CASSCF natural orbitals obtained for **TS7-S** revealed the presence of two orbitals with electron occupancies of 1.2563 and 0.7798, which are the positive and negative combinations of the π -type orbitals describing the unpaired electrons of the two HOO^\bullet units.

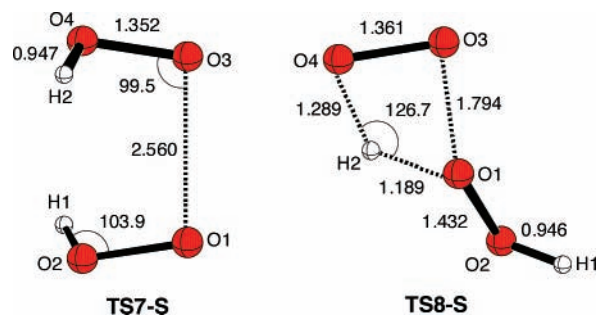


Figure 8. Selected geometrical parameters of the CASSCF/6-311+G(3df,2p)-optimized geometries of the transition structure (**TS7-S**) connecting the **CX1-S** complex with the **M1-S** minimum and the transition structure (**TS8-S**) connecting the **M3-S** minimum with the $2 + {}^1\text{O}_2$ products. Distances are given in Å and angles in deg.

Although the energy of **TS7-S** is calculated to be 1.8 kcal/mol lower than that of the isolated reactants, the formation of **M1-S** from **CX1-S** involves an energy barrier of 7.3 kcal/mol (see Table 1). These findings are in clear contrast with the results of the calculations by Zhu and Lin³⁴ predicting a barrierless formation of the H_2O_4 chain-structure adduct from the direct addition of two HOO^\bullet radicals. The failure of the B3LYP/6-311G(d,p) calculations in locating a transition structure for this reaction is ascribed to the inadequacy of the B3LYP method for dealing with species showing a large degree of multireference character.

The subsequent decomposition of **M1-S** yielding $2 + {}^1\text{O}_2$ involves the previous conversion of **M1-S** to **M3-S** via the rotational transition structure **TS6-S**, followed by the passage through a strained four-membered-ring transition structure, labeled as **TS8-S** (Figure 8). Zhu and Lin have also located at the UB3LYP/6-311G(d,p) level a transition structure (referred as TS3 in ref 34) for the decomposition of the H_2O_4 chain-structure intermediate yielding $\text{H}_2\text{O}_2 + {}^1\text{O}_2$. Although TS3 and **TS8-S** are qualitatively similar, the bond lengths of these transition structures are significantly different.

It is worth remarking that **TS8-S** involves the concerted breaking of two bonds (i.e., O1–O3 and H2–O4) and forming of a bond (i.e., O1–H2). As expected for such a strained structure, **TS8-S** is calculated to lie high in energy above the H_2O_4 tetraoxide intermediate. In fact, the decomposition of **M3-S** yielding $2 + {}^1\text{O}_2$ is predicted to involve an energy barrier of 45.2 kcal/mol (see Table 1), which is more than twice the value of 21.1 kcal/mol obtained by using the G2M(CC5) method.³⁴ It is likely that this discrepancy is due to the multireference character of **TS8-S** arising from the fact that this transition structure connects the closed-shell intermediate **M3-S** with the ${}^1\Delta_g$ open-shell singlet ${}^1\text{O}_2$. The present calculations indicate that the self-reaction of HOO^\bullet producing $\text{H}_2\text{O}_2 + {}^1\text{O}_2$ through a stepwise mechanism on the singlet PES requiring the

previous formation of a H₂O₄ tetraoxide intermediate is predicted to be energetically very unfavorable, as compared with the single H-atom transfer mechanism.

As regards the triplet PES, it was found that the geometry optimization of a H₂O₄ species with the HOOOH connectivity and triplet multiplicity leads to either the CX1-T complex or the 2 + ³O₂ products. Therefore, the H₂O₄ tetraoxide is not an energy minimum on the triplet PES. Consequently, any hypothetical stepwise mechanism for the self-reaction reaction of HOO• yielding H₂O₂ + ³O₂ based on the formation of a triplet H₂O₄ chain-structure intermediate can be discarded.

In summary, the present calculations suggest that the observed strong negative temperature dependence of the rate constant for reaction of eq 1 cannot be attributed to a stepwise mechanism involving the formation of a short-lived H₂O₄ intermediate with the HOOOH connectivity. Therefore, the observed strong negative temperature dependence should be ascribed to the reversible formation of the prereactive doubly hydrogen-bonded complex in the entrance channel. We have recently led to a similar conclusion for the CH₃OO• + HOO• reaction.⁶⁷

4. Summary and Conclusions

In an attempt to understand the mechanism of the gas-phase bimolecular self-reaction of HOO•, a key reaction in atmospheric environments, the singlet and triplet potential energy surfaces (PESs) for the gas-phase reaction between two HOO• radicals leading to HOOH + O₂ have been investigated by means of quantum-mechanical electronic structure methods (CASSCF and CASPT2). From the analysis of the results, the following main points emerge.

(1) All the reaction pathways on both PESs consist of a first step involving the barrierless formation of a prereactive doubly hydrogen-bonded complex, followed by the formation of the subsequent reaction products. This complex is a diradical species lying about 8 kcal/mol below the energy of the reactants at 0 K.

(2) The lowest energy reaction pathway on both PESs is a degenerate double hydrogen exchange between the HOO• moieties of the prereactive complex via a double proton transfer mechanism involving an energy barrier ranging from 1.1 kcal/mol (singlet) to 3.3 kcal/mol (triplet) at 0 K. Earlier theoretical studies on the self-reaction of HOO• have not considered such a low energy-barrier process.

(3) The single H-atom transfer between the two HOO• moieties of the prereactive complex, yielding HOOH and O₂, involves a conical intersection between either two singlet or two triplet states of A' and A'' symmetries if a plane containing the six atoms is maintained along the pathway. The lowest energy reaction pathway for this H-atom transfer occurs via a nonplanar *cisoid* transition structure. At 0 K, the energy barrier for this transition structure on the triplet PES is 5.8 kcal/mol, whereas that for the transition structure on the singlet PES is 17.5 kcal/mol. Therefore, the single H-atom transfer on the triplet PES is the dominant pathway for the self-reaction of HOO• leading to HOOH + O₂.

(4) The simple addition between the terminal oxygen atoms of the two HOO• moieties of the prereactive complex, leading to a covalently-bonded H₂O₄ adduct with the HOOOH connectivity on the singlet PES involves an energy barrier of 7.3 kcal/mol at 0 K. The decomposition of this intermediate into HOOH + ¹O₂ entails an energy barrier of 45.2 kcal/mol at 0 K. Furthermore, this H₂O₄ chain-structure species is not an energy minimum on the triplet PES. Consequently, the strong negative temperature dependence of the rate constant observed

for the self-reaction of HOO• leading to HOOH + O₂ cannot be attributed to the formation of a short-lived H₂O₄ intermediate with the HOOOH connectivity, but to the reversible formation of the prereactive doubly hydrogen-bonded complex in the entrance channel.

Acknowledgment. This research was supported by the Spanish MEC (Grants CTQ2005-07790 and UNBA05-33-001). Additional support came from the Catalonian AGAUR (Grants 2005SGR00111 and 2005PEIR0051/69). The larger calculations described in this work were performed at the Centre de Supercomputació de Catalunya (CESCA).

Supporting Information Available: Cartesian coordinates of all structures reported in this paper, a table summarizing total energies and zero-point vibrational energies, and a table giving the approximate tunneling factors. This material is available free of charge via the Internet at <http://pubs.acs.org>.

References and Notes

- (1) (a) Lightfoot, P. D.; Cox, R. A.; Crowley, J. N.; Destriau, M.; Hayman, G. D.; Jenkin, M. E.; Moortgat, G. K.; Zabel, F. *Atmos. Environ. Part A* **1992**, *26A*, 1805–1961. (b) Wallington, T. J.; Dagaut, P.; Kurrylo, M. J. *Chem. Rev.* **1992**, *92*, 667–710. (c) Lesclaux, R. Combination of peroxy radicals in the gas phase. In *Peroxy Radicals*; Alfassi, Z. B., Ed.; John Wiley & Sons: New York, 1997; pp 81–112.
- (2) (a) Lesko, T. M.; Colussi, A. J.; Hoffmann, M. R. *J. Am. Chem. Soc.* **2004**, *126*, 4432. (b) Lind, J.; Merenyi, E.; Brinck T. *J. Phys. Chem. A* **2003**, *107*, 676. (c) Sehested, K.; Corfitzen, H.; Holcman, J.; Hart, E. J. *J. Phys. Chem. A* **1998**, *102*, 2667.
- (3) Aust, A. E.; Eveleigh, J. F. *Proc. Soc. Exp. Biol. Med.* **1999**, *222*, 246.
- (4) Cox, R. A.; Burrows, J. P. *J. Phys. Chem.* **1979**, *83*, 2560.
- (5) Lii, R.-R.; Sauer, M. C., Jr.; Gordon, S. J. *Phys. Chem.* **1981**, *85*, 2833.
- (6) Sander, S. P.; Peterson, M.; Watson, R. T. *J. Phys. Chem.* **1982**, *86*, 1236.
- (7) Simonaitis, R.; Heicklein, J. *J. Phys. Chem.* **1982**, *86*, 3416.
- (8) Thrush, B. A.; Tyndall, G. S. *Chem. Phys. Lett.* **1982**, *92*, 232.
- (9) Baldwin, R. R.; Dean, C. E.; Honeyman, M. R.; Walker, R. W. *J. Chem. Soc., Faraday Trans.* **1984**, *80*, 3187.
- (10) Rozenshtein, V. B.; Gershenson, Yu. M.; Il'n, S. D.; Kishkovich, O. P. *Chem. Phys. Lett.* **1984**, *112*, 473.
- (11) Kurylo, M. J.; Ouellette, P. A.; Laufer, A. H. *J. Phys. Chem.* **1986**, *90*, 437.
- (12) Cox, R. A. *Chem. Rev.* **2003**, *103*, 4533–4548.
- (13) Hamilton, E. J., Jr. *J. Chem. Phys.* **1975**, *63*, 3682.
- (14) Hamilton, E. J., Jr.; Lii, R.-R. *Int. J. Chem. Kinet.* **1977**, *9*, 875.
- (15) Lii, R.-R.; Gorse, R. A., Jr.; Sauer, M. C., Jr.; Gordon, S. J. *Phys. Chem.* **1979**, *83*, 1803.
- (16) Lii, R.-R.; Gorse, R. A., Jr.; Sauer, M. C., Jr.; Gordon, S. J. *Phys. Chem.* **1980**, *84*, 813.
- (17) Sander, S. P.; Peterson, M.; Watson, R. T.; Patrick, R. *J. Phys. Chem.* **1982**, *86*, 1236.
- (18) Patrick, R.; Pilling, M. J. *Chem. Phys. Lett.* **1982**, *91*, 343.
- (19) Kircher, C. C.; Sander, S. P. *J. Phys. Chem.* **1984**, *88*, 2082.
- (20) Takacs, G. A.; Howard, C. J. *J. Phys. Chem.* **1986**, *90*, 687.
- (21) Lightfoot P. D.; Veyret, B.; Lesclaux, R. *J. Phys. Chem.* **1990**, *94*, 708.
- (22) Dobis, O.; Benson, S. W. *J. Am. Chem. Soc.* **1993**, *115*, 8798.
- (23) Maricq, M. M.; Szente, J. J. *J. Phys. Chem.* **1994**, *98*, 2078.
- (24) Christensen, L. E.; Okuma, M.; Sander, S. P.; Salawitch, R. J.; Toon, G. C.; Sen, B.; Blavier, J.-F.; Jucks, K. W. *Geophys. Res. Lett.* **2002**, *29*, art. no. 1299.
- (25) Bloss, W. J.; Rowley, D. M.; Cox, R. A.; Jones, R. L. *Phys. Chem. Chem. Phys.* **2002**, *4*, 3639.
- (26) Kappel, Ch.; Luther, K.; Troe, J. *Phys. Chem. Chem. Phys.* **2002**, *4*, 4392.
- (27) Stone, D.; Rowley, D. M. *Phys. Chem. Chem. Phys.* **2005**, *7*, 2156.
- (28) Patrick, R.; Barker, J. R.; Golden, D. M. *J. Phys. Chem.* **1984**, *88*, 128.
- (29) Mozurkewich, M.; Benson, S. W. *Int. J. Chem. Kinet.* **1985**, *17*, 787.
- (30) Lightfoot, P. D.; Veyret, B.; Lesclaux, R. *Chem. Phys. Lett.* **1988**, *150*, 120.
- (31) Fitzgerald, G.; Schaefer, H. F., III. *J. Chem. Phys.* **1984**, *81*, 362.

- (32) Fitzgerald, G.; Lee, T. J.; Bartlett, R. J.; Schaefer, H. F., III. *J. Chem. Phys.* **1985**, *83*, 6275.
- (33) Fermann, J. T.; Hoffman, B. C.; Tschumper, G. S.; Schaefer, H.F., III. *J. Chem. Phys.* **1997**, *106*, 5102.
- (34) Zhu, R. S.; Lin, M. C. *Phys. Chem. Commun.* **2001**, *4*, 106.
- (35) Mebel, A. M.; Morokuma, K.; Lin, M. C. *J. Chem. Phys.* **1995**, *103*, 7414.
- (36) Koch, W.; Holthausen, M. C. *A Chemist's Guide to Density Functional Theory*; Wiley-VCH: Weinheim, Federal Republic of Germany, 2000; pp 248–250.
- (37) Donaldson, D. J.; Francisco, J. S. *Phys. Chem. Chem. Phys.* **2003**, *5*, 3183.
- (38) For a review, see: Roos, B. O. *Adv. Chem. Phys.* **1987**, *69*, 399.
- (39) Frisch, M. J.; Pople, J. A.; Binkley, J. S. *J. Chem. Phys.* **1984**, *80*, 3265.
- (40) Hehre, W. J.; Radom, L.; Schleyer, P. v. R.; Pople, J. A. *Ab Initio Molecular Orbital Theory*; John Wiley: New York, 1986; pp 86–87.
- (41) Schlegel, H. B. *J. Comput. Chem.* **1982**, *3*, 214.
- (42) Bofill, J. M. *J. Comput. Chem.* **1994**, *15*, 1.
- (43) Anglada, J. M.; Bofill, J. M. *Theor. Chim. Acta* **1995**, *92*, 369.
- (44) (a) Fukui, K. *Acc. Chem. Res.* **1981**, *14*, 363. (b) Ishida, K.; Morokuma, K.; Kormornicki, A. *J. Chem. Phys.* **1977**, *66*, 2153.
- (45) (a) Gonzalez, C.; Schlegel, H. B. *J. Chem. Phys.* **1989**, *90*, 2154. (b) Gonzalez, C.; Schlegel, H. B. *J. Phys. Chem.* **1990**, *94*, 5523.
- (46) (a) Anglada, J. M.; Bofill, J. M. *J. Comput. Chem.* **1997**, *18*, 992. (b) De Vico, L.; Olivucci, M.; Lindth, R. *J. Chem. Theory Comput.* **2005**, *1*, 1029.
- (47) (a) Anderson, K.; Malmqvist, P.-A.; Roos, B. O.; Sadlej, A. J.; Wolinski, K. *J. Phys. Chem.* **1990**, *94*, 5483. (b) Anderson, K.; Malmqvist, P.-A.; Roos, B. O. *J. Chem. Phys.* **1992**, *96*, 1218.
- (48) Boys, S. F.; Bernardi, F. *Mol. Phys.* **1970**, *19*, 553.
- (49) Bader, R. F. W. *Atoms in Molecules: A Quantum Theory*; Clarendon: Oxford, U.K., 1990.
- (50) Schmidt, M. W.; Baldrige, K. K.; Boatz, J. A.; Elbert, S. T.; Gordon, M. S.; Jensen, J.; Koseki, S.; Matsunaga, N.; Nguyen, K. A.; Su, S.; Windus, T. L.; Dupuis, M.; Montgomery, J. A. *J. Comput. Chem.* **1993**, *14*, 1347.
- (51) Karlström, G.; Lindh, R.; Malmqvist, P.-Å.; Roos, B. O.; Ryde, U.; Veryazov, V.; Widmark, P.-O.; Cossi, M.; Schimmelpfennig, B.; Neogrady, P.; Seijo, L. *Comput. Mater. Sci.* **2003**, *28*, 222.
- (52) (a) Biegler-König, F. W.; Bader, R. F. W.; Tang, T.-H. *J. Comput. Chem.* **1982**, *3*, 317. (b) Bader, R. F. W.; Tang, T.-H.; Tal, Y.; Biegler-König, F. W. *J. Am. Chem. Soc.* **1982**, *104*, 946.
- (53) Wigner, E. *Z. Phys. Chem. B* **1932**, *148*, 241.
- (54) NIST Chemistry Webbook (<http://webbook.nist.gov/chemistry>).
- (55) Francisco, J. S.; Zhao, Y. *Mol. Phys.* **1991**, *72*, 1207.
- (56) Lubic, K. G.; Amano, T. *J. Chem. Phys.* **1984**, *81*, 4826.
- (57) Cremer, D. General and theoretical aspects of the peroxide group. In *The Chemistry of Functional Groups. Peroxides*; Patai, S., Ed.; John Wiley & Sons: New York, 1983; pp 1–84.
- (58) Herzberg, G. *Spectra of Diatomic Molecules*, 2nd ed.; McGraw Hill: New York, 1950.
- (59) See, e.g.: McQuarrie, D. *Statistical Mechanics*; Harper and Row: New York, 1986.
- (60) Tyndall, G. S.; Cox, R. A.; Granier, C.; Lesclaux, R.; Moortgat, G. K.; Pilling, M. J.; Ravishankara, A. R.; Wallington, T. J. *J. Geophys. Res.* **2001**, *106*, 12157–12182.
- (61) (a) Cremer, D. *Croat. Chem. Acta* **1984**, *57*, 1259. (b) Cremer, D. *Angew. Chem., Int. Ed. Engl.* **1984**, *23*, 627.
- (62) Anglada, J. M. *J. Am. Chem. Soc.* **2004**, *126*, 9809.
- (63) Anglada, J. M.; Olivella, S.; Solé, A. *J. Phys. Chem. A* **2006**, *110*, 1982.
- (64) Goddard, W. A., III; Dunning, T. H.; Hunt, W. J.; Hay, P. J. *Acc. Chem. Res.* **1973**, *6*, 368.
- (65) Although the **CI-S** and **CI-T** structures have C_s symmetry, the geometry optimization of both conical intersections was carried out without imposing any symmetry constraint.
- (66) Bofill, J. M.; Olivella, S.; Sole, A.; Anglada, J. M. *J. Am. Chem. Soc.* **1999**, *121*, 1337.
- (67) Anglada, J. M.; Olivella, S.; Solé, A. *J. Phys. Chem. A* **2006**, *110*, 6073.